Supplementary material for manuscript:

Metallomacrocycles as anion receptors: combining hydrogen bonding and ion pair based hosts formed from Ag(I) salts and flexible bis- and tris-pyrimidine ligands.

Andres Tasada,[a] Francisca M. Albertí,[a] Antonio Bauzá,[a] Miquel Barceló-Oliver,[a] Angel García-Raso,*[a] Juan J. Fiol,[a] Elies Molins,[b] Amparo Caubet[c] and Antonio Frontera*[a]

Table of contents:

Materials and methods	**Pag 2**
Synthesis of L^1	**Pag 2**
Synthesis of L^2	**Pag 2**
Synthesis of NO_3^-@H^1	**Pag 2**
Synthesis of BF_4^-@H^1	**Pag 2**
Synthesis of TsO^-@H^1	**Pag 2**
Synthesis of NO_3^-@H^2	**Pag 2**
Synthesis of BF_4^-@H^2	**Pag 3**
Data collection and refinement	**Pag 3**
ORTEP images and description of the structures	**Pag 3**
Computational details	**Pag 7**
Theoretical analysis, results and discussion	**Pag 7**
References	**Pag 8**

Materials and methods

Elemental microanalyses were carried out using a Carlo Erba model 1108 or a Thermo Finnigan model Flash EA 1112 microanalyzers. IR spectra in the solid state (KBr or CsI pellets) were measured on a Bruker IFS 66 spectrometer. NMR spectra were recorded on a Bruker AMX300 spectrophotometer at room temperature. ^{1}H chemical shifts in deuterated dimethyl sulfoxide (DMSO-d_6) were referenced to DMSO-d_6 [^{1}H-NMR, δ(DMSO = 2.47 ppm]. Reagents were used as received from Sigma-Aldrich.

Synthesis of L^1

The synthesis of this ligand has been performed using the previously reported methodology:[1] a suspension of 2-chloropyrimidine (1.1 g, 9.6 mmol) in n-butanol (20 ml) and triethylamine (3 ml) were refluxed with the stoichiometric amount of propane-1,3-diamine (4.8 mmol) during 4 h. The resulting solids were filtered off and washed with cold water and cold acetone to remove the impurities of triethylammonium hydrochloride that contaminate the crude materials. Further purification can be achieved by recrystallisation from boiling water.

Synthesis of L^2

A suspension of 2-chloropyrimidine (1.4 g, 12 mmol) in n-butanol (20 ml) and triethylamine (3 ml) were refluxed with 1,4,7-triazaheptane (0.3 g, 3 mmol) during 24 h. The resulting reaction crude is treated with and excess of ammonium hydroxide and the solvent is eliminated under vacuum. The resulting solid is washed with water and filtered off, obtaining the desired product (58% yield). Anal. Found: C, 56.60; H, 5.73; N, 37.13 %. Calc. for $C_{16}H_{19}N_9$: C, 56.96; H, 5.68; N, 37.36 %. IR (cm^{-1}): 3258s, 3046s, 2940s, 1615vs, 1583vs, 1545vs, 1500vs, 1463vs, 1440s, 1423vs, 1380s, 1367s, 1315m, 1283m, 1244m, 1216w, 1178m, 1154w, 1125w, 1089w, 1070w, 996m, 850w, 801s,766m, m, 642m, 612w, 523w, 502m. *^{1}H NMR (DMSO-d_6)*: δ (ppm) 8.29 d [2H, H(10)/H(12), J = 4.5 Hz], 8.17 d [4H, H(4)/H(6)/H(4')/H(6'), J = 4.8 Hz], 7.14 br t [2H, N-H], 6.56 t [1H, H(11), J = 4.8 Hz], 6.49 t [2H, H(5)/H(5'), J = 4.8 Hz], 3.70 br t [4H, H(14)/H(14'), J = 6.3 Hz], 3.45 br m [4H, H(13)/H(13')]. *^{13}C RMN, δ(DMSO-d_6):* 162.7 [C(2)/C(2')], 161.7 [C(8)], 158.3 [C(4)/C(6)/C(4')/C(6')], 158.2 [C(10)/C(12)], 110.4 [C(5)/C(5')], 110.1 [C(11)], 47.6 [C(14)/C(14')].

Synthesis of $2NO_3^-$@H^1:

1.75 mmol of $AgNO_3$ are added to a solution of 0.5 mmol of $\mathbf{L^1}$ in 20 ml of HNO_3 0.05 M. The resulting solution was refluxed during 1h, filtered and allowed to slowly evaporate at room temperature and light-protected. This large excess of $AgNO_3$ is required to obtain suitable crystals for X-ray crystallography after several weeks (35% yield).
Anal. Found: C, 18.06; H, 1.72; N, 17.03 %. Calc. for $C_{11}H_{14}Ag_3N_9\ O_9$: C, 17.86; H, 1.91; N, 17.04 %. IR (cm^{-1}): 3257m, 1596s, 1540s, 1460s, 1383vs, 1293s, 1265s, 1174m, 1078w, 1032w, 991m, 825m, 800m, 783m, 633w, 642w, 518w, 480w.

Synthesis of $2BF_4^-$@H^1:

0.25 mmol of $AgBF_4$ are added to a solution of 0.5 mmol of $\mathbf{L^1}$ in 20 ml of water. The resulting solution was refluxed during 1h, filtered and allowed to slowly evaporate at room temperature and light-protected. Suitable crystals for X-ray crystallography are obtained in very low yield. For this complex the reflux has been carried out in standard glassware since the formation of undesired products like BF_3OH^- and SiF_6^{2-} has not been detected after 1h of refluxing conditions. As a matter of fact the ν(SiF) peak has not been detected in the IR spectrum and the XRPD patterns of the bulk sample and the single crystals are equivalent.
Anal. Found: C 31.59; H 3.86; N 20.27% . Calc. for $C_{11}H_{14}AgBF_4N_6$: C 31.09; H 3.32, N 19.78%. IR (cm^{-1}): 3389m, 3263s, 3107m, 2941m, 2877m, 1597vs, 1575vs, 1536vs, 1454vs, 1417s, 1363s, 1332s, 1265s, 1221m, 1175m, 1115-1035 br b, 991s, 799s, 774 m, 741m, 643m.

Synthesis of $2TsO^-$@H^1:

0.25 mmol of AgTsO are added to a solution of 0.5 mmol of $\mathbf{L^1}$ in 20 ml of water. The resulting solution was refluxed during 1h, filtered and allowed to slowly evaporate at room temperature and light-protected. Suitable crystals for X-ray crystallography are obtained after one week (42% yield).
Anal. Found: C, 42.69; H, 4.11; N, 16.67%. Calculado para $C_{18}H_{21}AgN_6O_3S$: C, 42.45; H, 4.16; N, 16.50%. IR (cm^{-1}): 3315m, 2919m, 1597vs, 1573vs, 1537s, 1465m, 1418s, 1365s, 1353s, 1270m, 1247, 1202vs, 1189vs, 1120s, 1088m, 1045m, 1032m, 1009s, 824m, 815m, 795s, 777m, 750w, 680s, 566s.

Synthesis of $2NO_3^-$@H^2:

1.76 mmol of $AgNO_3$ are added to a solution of 0.3 mmol of $\mathbf{L^2}$ in 20 ml of HNO_3 0.05 M. The resulting solution was refluxed during 1h, filtered and allowed to slowly evaporate at room temperature and light-protected. This large excess of $AgNO_3$ is required to obtain suitable crystals for X-ray crystallography, which are formed after few days (40% yield).
Anal. Found: C, 23.49; H, 2.29; N, 19.84%. Calc. for $C_{16}H_{19}Ag_3N_{12}O_9$: C, 22.69; H, 2.26; N, 19.84%. IR (cm^{-1}

[1]): 3257m, 3074m, 1602vs, 1547vs, 1511s, 1455s, 1382br vs, 1318s, 1301s, 1282s, 1244s, 1170s, 1105m, 1034m, 997m, 995s, 864m, 816m, 786s, 655m, 505m.

Synthesis of $2BF_4^-$@H^2:

0.4 mmol of $AgBF_4$ are added to a solution of 0.6 mmol of $\mathbf{L^1}$ in 20 ml of water. The resulting solution was refluxed during 1h, filtered and allowed to slowly evaporate at room temperature and light-protected. Suitable crystals for X-ray crystallography are obtained after few days (27% yield). For this complex the reflux has been carried out in standard glassware since the formation of undesired products like BF_3OH^- and SiF_6^{2-} has not been detected after 1h of refluxing conditions. As a matter of fact the ν(SiF) peak has not been detected in the IR spectrum and the XRPD patterns of the bulk sample and the single crystals are equivalent.
Anal. Found: C 34.70; H 4.16; N 22,38%. Calc. for $C_{32}H_{42}Ag_2B_2F_8N_{18}O_2$ C 34.94; H 3.85, N 22,92%. IR (cm^{-1}): 3260s, 3096m, 1607vs, 1584vs, 1546vs, 1503s, 1469s, 1425s, 1381s, 1319m, 1281m, 1245m, 1178m, 1084 br b, 995s, 796s.

Crystal data collection and refinement

Suitable crystals of all the compounds were glued at the tip of a glass fibre and mounted on an Enraf-Nonius CAD4 diffractometer with graphite monochromator and a Mo-Kα sealed tube (λ = 0.71073 Å). Cell parameters were determined from a set of 25 randomly searched reflections. Data were collected at room temperature using ω-2θ scans. XCAD4[2] and DIFABS,[3] both included in the WinGX[4] suite, were used for data reduction and empirical absorption correction, respectively (except for $\mathbf{2BF_4^-@H^2}$, for which ψ-scan empirical absorption corrections[5] were applied).

Solving for structure factor phases was performed by direct methods using SHELXS97[6] ($\mathbf{2NO_3^-@H^1}$), SIR97[7] ($\mathbf{2BF_4^-@H^2}$), SIR2002[8] ($\mathbf{2BF_4^-@H^1}$ and $\mathbf{2NO_3^-@H^2}$) or SIR2004[9] ($\mathbf{2TsO^-@H^1}$) and the full-matrix least-squares refinement on F^2, by SHELXL97.[6] The structures were checked for higher symmetry with the aid of the program PLATON.[10] Non-H atoms were refined anisotropically and H-atoms were introduced in calculated positions and refined riding on their parent atoms.
Crystallographic data: $C_{22}H_{28}Ag_6N_{18}O_{18}$ ($\mathbf{2NO_3^-@H^1}$), M_r = 1479.84, monoclinic, $P2_1/c$, a = 8.368(3), b = 7.7000(10), c = 29.646(17) Å, β = 94.91(4)°, V = 1903.2(13) Å^3, Z = 2, ρ_c = 2.582 Mg m^{-3}, T = 294(2) K, λ = 0.71073 Å. 4227 independent reflections [R(int) = 0.0262], used in all calculations. R_1 = 0.0524, wR_2 = 0.1447 for $I > 2\sigma(I)$, and R_1 = 0.0568, wR_2 = 0.1480 for all unique reflections. Max./min. residual electron densities 1.009 and –1.529 e Å^{-3}. Deposition number: CCDC 921145.
$C_{11}H_{14}AgBF_4N_6$ ($\mathbf{2BF_4^-@H^1}$), M_r = 424.96, monoclinic, $P2_1/c$, a = 4.798(6), b = 13.756(2), c = 22.487(3) Å, β = 93.377(11)°, V = 1481.6(19) Å^3, Z = 4, ρ_c = 1.905 Mg m^{-3}, T = 294(2) K, λ = 0.71073 Å. 2674 independent reflections [R(int) = 0.0251], used in all calculations. R_1 = 0.0392, wR_2 = 0.0982 for $I > 2\sigma(I)$, and R_1 = 0.0551, wR_2 = 0.1109 for all unique reflections. Max./min. residual electron densities 0.8200 and –1.082 e Å^{-3}. Deposition number: CCDC 921146.
$C_{36}H_{42}Ag_2N_{12}O_6S_2$ ($\mathbf{2TSO^-@H^1}$), M_r = 1018.68, monoclinic, $P2_1/c$, a = 12.611(2), b = 11.643(2), c = 14.3923(19) Å, β = 112.081(13)°, V = 1958.2(5) Å^3, Z = 2, ρ_c = 1.728 Mg m^{-3}, T = 294(2) K, λ = 0.71073 Å. 3427 independent reflections [R(int) = 0.0111], used in all calculations. R_1 = 0.0284, wR_2 = 0.0752 for $I > 2\sigma(I)$, and R_1 = 0.0352, wR_2 = 0.0776 for all unique reflections. Deposition number: CCDC 921147.
$C_{16}H_{19}Ag_3N_{12}O_9$ ($\mathbf{2NO_3^-@H^2}$), M_r = 847.04, triclinic, P-1, a = 7.310(4), b = 10.068(7), c = 17.074(13) Å, α = 101.53(6)°, β = 96.20(5)°, γ = 104.51(6)°, V = 1175.3(15) Å^3, Z = 2, ρ_c = 2.394 Mg m^{-3}, T = 294(2) K, λ = 0.71073 Å. 4127 independent reflections [R(int) = 0.0429], used in all calculations. R_1 = 0.0490, wR_2 = 0.1312 for $I > 2\sigma(I)$, and R_1 = 0.0524, wR_2 = 0.1343 for all unique reflections. Max./min. residual electron densities 1.436 and –1.610 e Å^{-3}. Deposition number: CCDC 921148.
$C_{32}H_{46}Ag_2B_2F_8N_{18}O_4$ ($\mathbf{2BF_4^-@H^2}$), M_r = 1136.23, triclinic, P-1, a = 10.874(5), b = 11.150(5), c = 11.523(4) Å, α = 96.688(14)°, β = 117.81(3)°, γ = 108.686(5)°, V = 1110.0(9) Å^3, Z = 1, ρ_c = 1.700 Mg m^{-3}, T = 294(2) K, λ = 0.71069 Å. 9603 independent reflections [R(int) = 0.0146], used in all calculations. R_1 = 0.0540, wR_2 = 0.1568 for $I > 2\sigma(I)$, and R_1 = 0.0908, wR_2 = 0.1775 for all unique reflections. Max./min. residual electron densities 1.561 and –1.508 e Å^{-3}. Deposition number: CCDC 921149.

ORTEP images and description of the structures

The $\mathbf{2NO_3^-@H^1}$ complex (Fig. S1) forms a $L_2Ag_2^{2+}$ 20-member nearly planar macrocycle by linear coordination of two Ag(I) ions with the pyrimidine rings of two different ligands that lies about an inversion centre. Two nitrate anions are placed on top and bottom and form hydrogen bonds with the N-H groups directed inside the cycle, as has been discussed along the paper. The macrocyclic complex forms a piling plane by means of stacking interactions and $CH_{(pir)}\cdots O_{(nitrate)}$ hydrogen bonds. Four additional Ag(I) ions coordinate the rest of pyrimidine nitrogen atoms and interact with other nitrate anions. The external silver nitrate bi-dimensional net is responsible of the formation of the 3D structure.

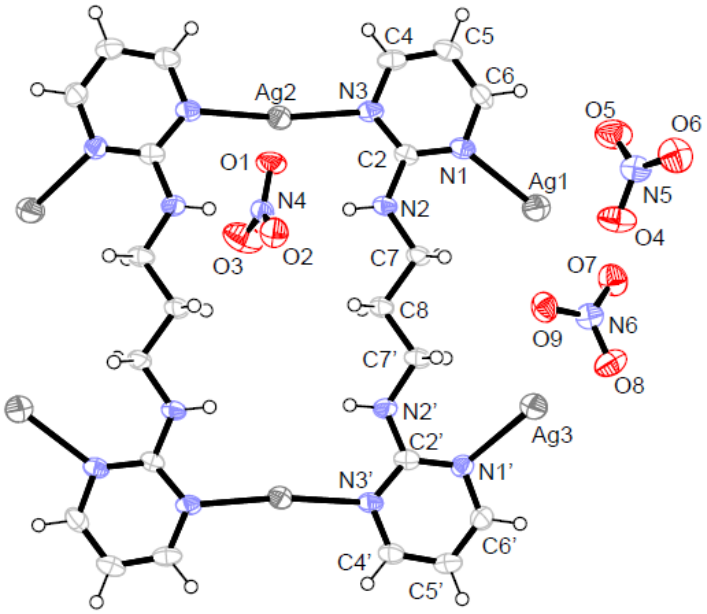

Fig. S1 ORTEP representation of **$2NO_3^-$@H[1]** drawn at the 50% probability level.

The **$2BF_4^-$@H[1]** shapes an infinite chain of alternating ligands and Ag(I) ions in the solid state (Fig. S2). The environment coordination of the Ag(I) ions is produced by the linear union to pyrimidines of two different ligands in a nearly orthogonal disposition. The coordination sphere of silver ions is completed with additional bonds to three different BF_4^- anions which are stabilised by hydrogen bonds with the NH groups of the ligands and an additional anion-π interaction.

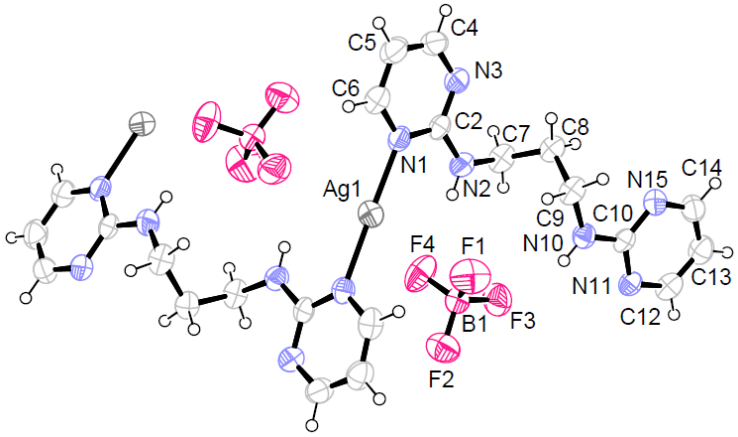

Fig. S2 ORTEP representation of **$2BF_4^-$@H[1]** drawn at the 50% probability level.

In the **$2TsO^-$@H[1]** complex (Fig. S3) a distorted 20-member macrocycle is created by two Ag(I) ions in a nearly linear coordination with the pyrimidine rings of two different ligands that lies about an inversion centre. Two tosilato anions directly coordinated to the Ag(I) ions are placed on top and bottom of the cycle forming hydrogen bonds with the N-H groups. Additional Ag···O interactions are observed both the encapsulated anions and with other anions belonging to neighbouring macrocycles. Intermolecular hydrogen bonds and stacking interactions yield to the formation of a three-dimensional structure for this compound.

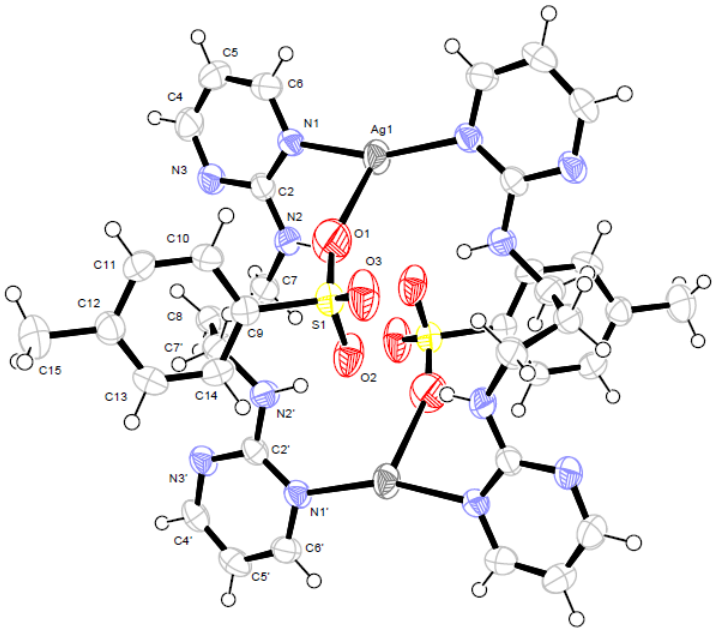

Fig. S3 ORTEP representation of **2TsO⁻@H[1]** drawn at the 50% probability level.

The **2NO$_3^-$@H[2]** complex (Fig. S4) forms a 24-member macrocycle with two Ag(I) ions in an distorted linear coordination with the four ending pyrimidine moieties of two different ligands about a plane that lies about an inversion centre. These pyrimidine rings are also linked with four additional Ag(I) ions to the central pyrimidine rings placed parallel outside the plane generating additional 9-member cycles. Two nitrate anions establish hydrogen bonds with the N-H groups and act as bridges between macrocycles, being linked to the Ag(I) ions. Moreover, the different macrocycles interact via another bridging nitrate anions with the outside Ag(I) ions producing infinite chains. Stacking and CH···O$_{(nitrate)}$ interactions are also observed. In contrast to **2NO$_3^-$@H[1]** complex described above, the nitrate anions that are recognized by the N–H groups of the host are bonded to silver ions belonging to two neighbouring macrocycles (see Fig S5, right). Both structures are compared in Fig. S5, where the two different recognition modes can be appreciated. This recognition pattern is responsible of the piling of the cycles in an infinite ladder. On the other hand, outside bound silver atoms do not form a silver nitrate net, as they do in **2NO$_3^-$@H[1]** complex. Instead of this, they form silver nitrate lines, which are responsible of the final packing of the structure.

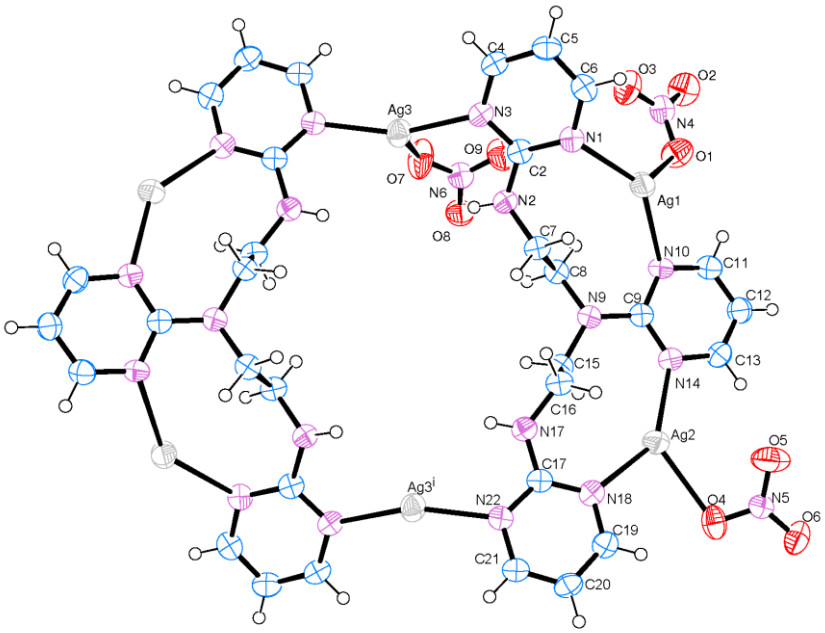

Fig. S4 ORTEP representation of **2NO$_3^-$@H[2]** drawn at the 50% probability level. Symmetry operator for generating equivalent atoms: (i), -x, -y, 1-z

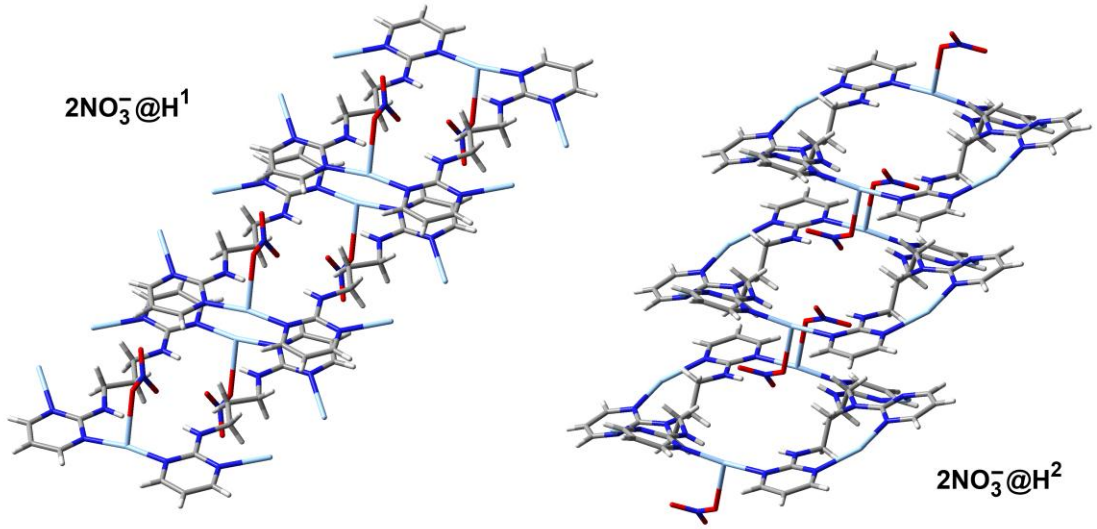

Fig. S5 Partial views of the X-ray structures of **$2NO_3^-$@H^1** (left) and **$2NO_3^-$@H^2** (right).

The **$2BF_4^-$@H^2** complex (Fig. S6) consists of a 24-member macrocycle similar to **$2NO_3^-$@H^2**, where two Ag(I) ions form the macrocycle with an approximately linear coordination with the four ending pyrimidine moieties of two different ligands. Moreover, the macrocycle lies about an inversion centre. Two water molecules are placed on top and bottom connecting the N-H groups of the macrocycle cycle with both tetrafluorborate anions. Additional Ag···Ag interactions between macrocycles are observed. Stacking between pyrimidines of different macrocycles allow the formation of planes while anions and water molecules between planes produce CH···F and CH···O_w interactions.

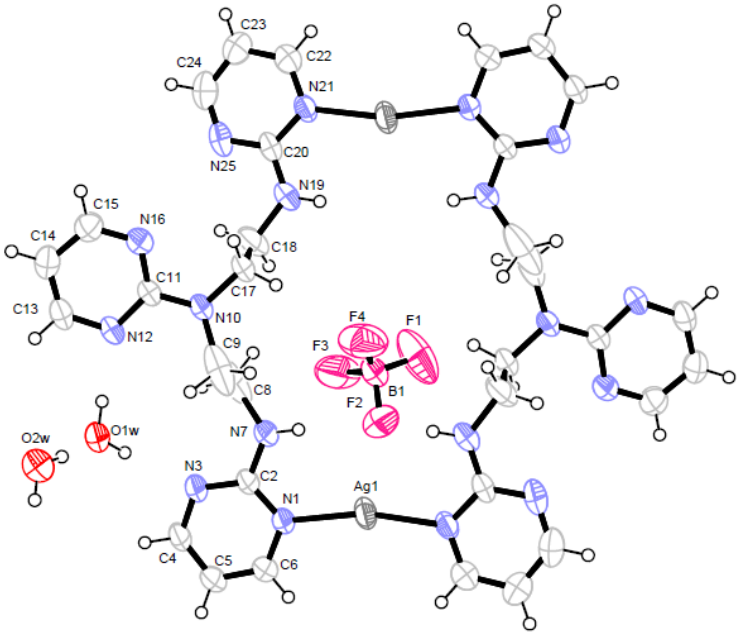

Fig. S6 ORTEP representation of **$2BF_4^-$@H^2** drawn at the 50% probability level.

Table S1. Size of cycles (or chain in **$2BF_4^-@H^1$**)

Complex	d[Ag···Ag] (Å)	d[NH···HN] (Å)
$2NO_3^-@H^1$	9.11	4.73 3.44
$2BF_4^-@H^1$	7.53	3.51
$2TsO^-@H^1$	6.97	3.39 3.78
$2NO_3^-@H^2$	9.53	5.60 3.86
$2BF_4^-@H^2$	10.06	5.87 3.52

Computational details

All calculations were carried out using the Turbomole package version 6.4[11] using the BP86-D3/def2-TZVPD method, which includes the latest available correction for dispersion.[12] All geometries (hosts, guests and complexes) have been fully optimized without symmetry constrains. Solvent effects have been evaluated by means of the COSMO (Conductor Like Screening Model) approximation using water as solvent.[13]

Theoretical analysis, results and discussion

The interaction energies of both hosts complexed to either one or two anions are gathered in Table S2. Moreover, all optimized complexes are represented in Figs. S7-S12. We have computed the interaction energies in vacuum and water using a continuum model. The interaction energies are large and negative for all complexes. The tetrahedral anions $BF4^-$ and TsO^- have more preference for **H^1** than the trigonal planar NO_3^- ion. This preference is not observed for **H^2** since BF_4^- and NO_3^- have similar interaction energies. For both hosts the TsO^- anion presents the most favorable binding energy due to additional π–π stacking interactions (see Fig. S7). For complexes with two anions the energetic results indicate that the BF_4^- ion forms the less favorable complexes, likely due to its low coordination ability. In fact the anions are located at more that 3.0 Å from the metal centers.

Table S2. Binding energies in vacuum and water solvent. Values in kcal/mol.

Complex	**E_{vacuum}**	**E_{water}**	**Complex**	**E_{vacuum}**	**E_{water}**
$NO_3^-@H^1$	-106.6	-22.3	**$2NO_3^-@H^1$**	-252.7	-31.3
$NO_3^-@H^2$	-159.9	-28.5	**$2NO_3^-@H^2$**	-246.9	-35.4
$BF_4^-@H^1$	-154.8	-19.4	**$2BF_4^-@H^1$**	-234.1	-24.2
$BF_4^-@H^2$	-153.2	-26.6	**$2BF_4^-@H^2$**	-229.8	-30.5
$OTs^-@H^1$	-188.5	-44.6	**$2OTs^-@H^1$**	-279.0	-51.6
$OTs^-@H^2$	-176.3	-50.3	**$2OTs^-@H^2$**	-271.0	-68.2

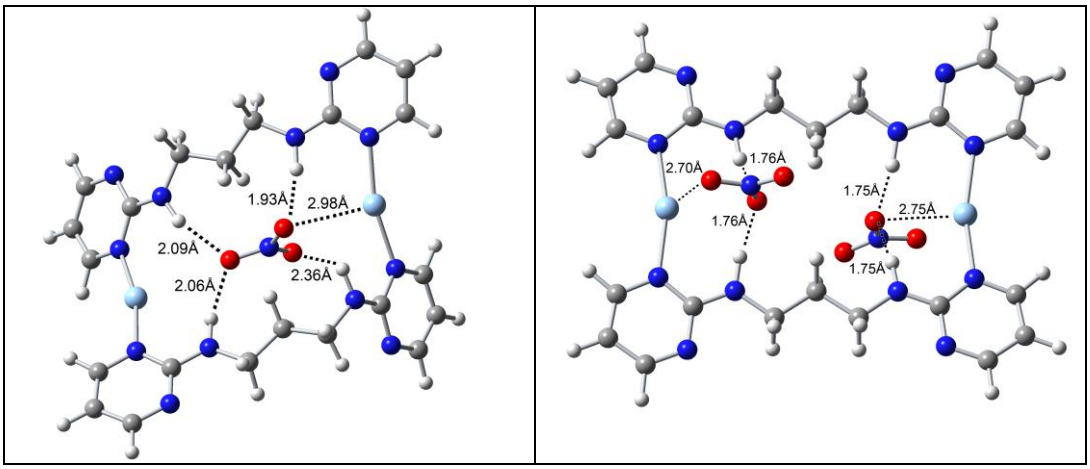

Fig. S7 NO_3^- mono and dicoordinated complexes with host **H^1**.

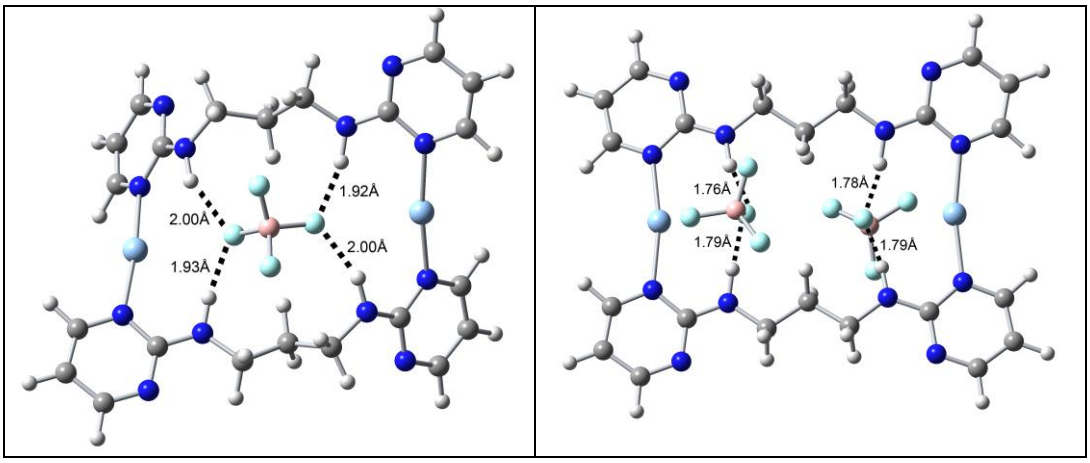

Fig. S8 BF_4^- mono and dicoordinated complexes with host $\mathbf{H^1}$.

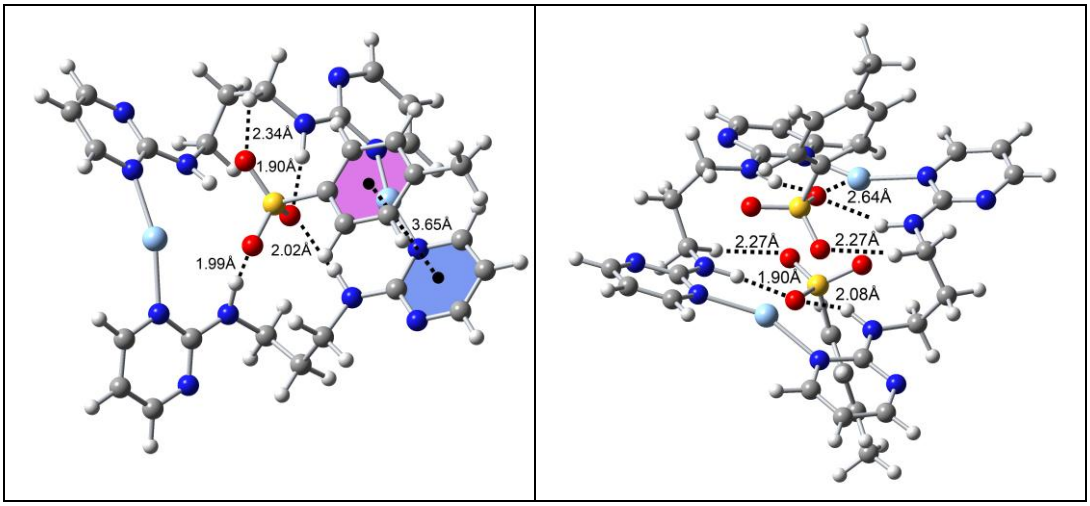

Fig. S9 TsO^- mono and dicoordinated complexes with host $\mathbf{H^1}$.

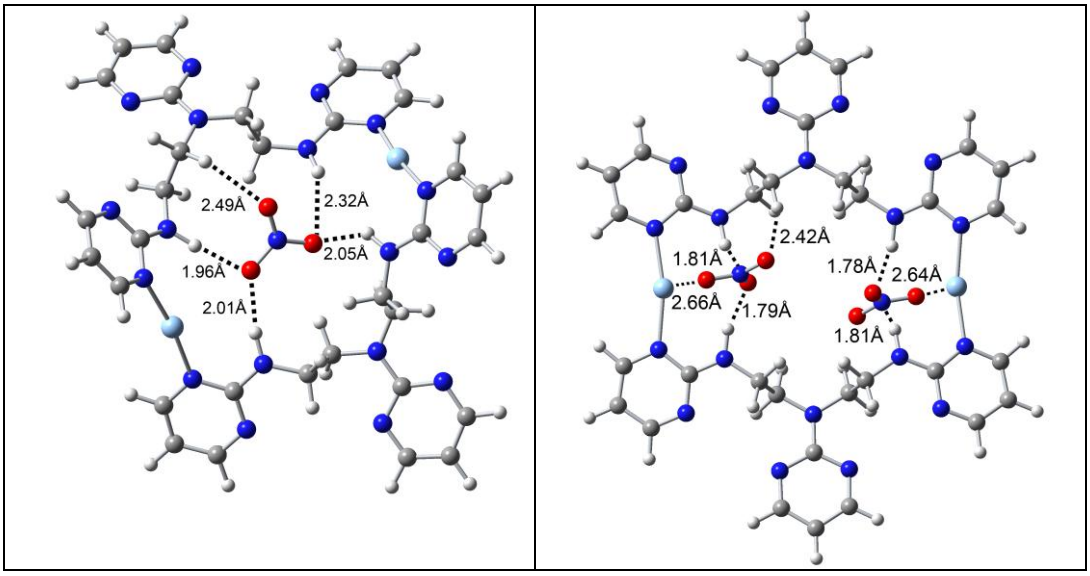

Fig. S10 NO_3^- mono and dicoordinated complexes with host $\mathbf{H^2}$.

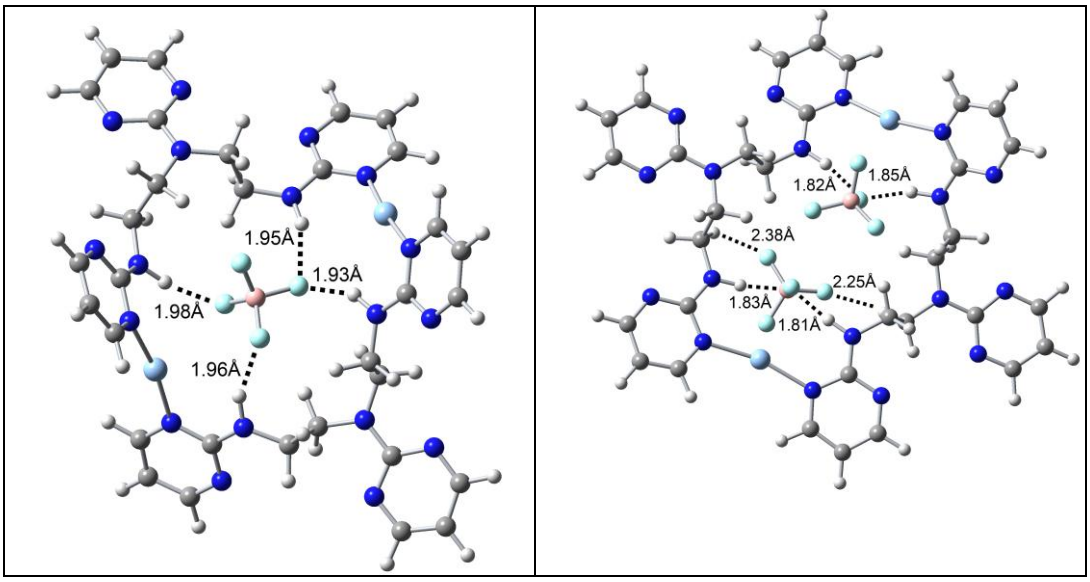

Fig. S11 BF_4^- mono and dicoordinated complexes with host $\mathbf{H^2}$.

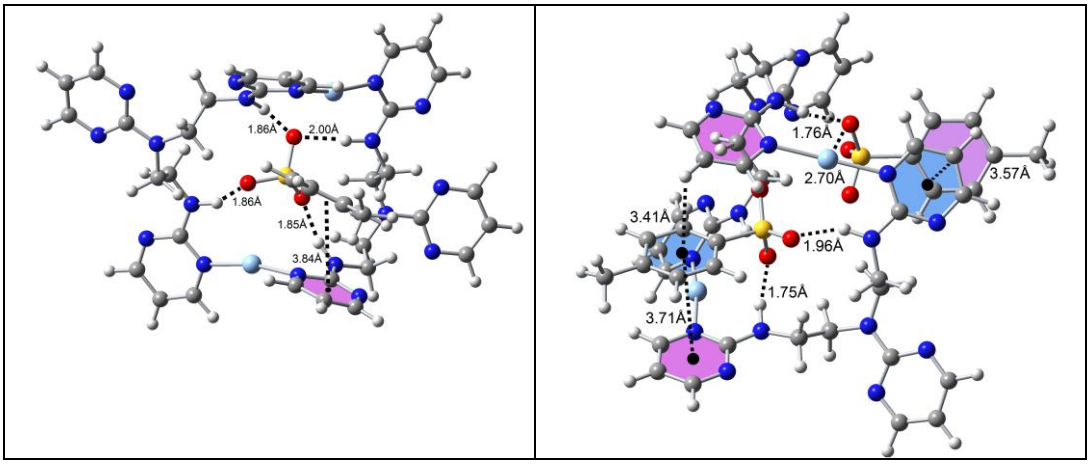

Fig. S12 TsO^- mono and dicoordinated complexes with host $\mathbf{H^2}$.

References

1 A. García-Raso, J. J. Fiol, A. Tasada, F. M. Albertí, E. Molins, M. G. Basallote, M. A. Máñez, M. J. Fernández-Trujillo and D. Sánchez, *Dalton Trans*., 2005, **23**, 3763.
2 CAD4 Data Reduction, K. Harms and S. Wocadlo, University of Marburg, Marburg, Germany, 1995.
3 N. Walker and D. Stuart, *Acta Crystallogr., Sect. A: Found. Crystallogr*., 1983, **39**, 158.
4 L. J. Farrugia, *J. Appl. Crystallogr.*, 1999, **32**, 837.
5 A.C.T North, D. C Phillips,. F. S. Mathews, Acta Crystallogr. Sect. A, 24 (1968) 351-359.
6 G.M. Sheldrick, *Acta Crystallogr., Sect. A: Found. Crystallogr*., 2008, **64**, 112.
7 A. Altomare, M.C. Burla, M. Camalli, G.L. Cascarano, C. Giacovazzo, A. Guagliardi, A.G.G. Moliterni, G. Polidori and R. Spagna, *J. Appl. Cryst.*, 1999, **32**, 115.
8 M.C. Burla, M. Camalli, B. Carrozzini, G.L. Cascarano, C. Giacovazzo, G. Polidori and R. Spagna, *J. Appl. Cryst.*, 2003, **36**, 1103.
9 M.C. Burla, R. Caliandro, M. Camalli, B. Carrozzini, G.L. Cascarano, L. De Caro, C. Giacovazzo, G. Polidori and R. Spagna, *J. Appl. Crystallogr.*, 2005, **38**, 381.
10 A.L. Spek, *J. Appl. Crystallogr.*, 2003, **36**, 7.
11 R. Ahlrichs, M. Bär, M. Hacer, H. Horn and C. Kömel, *Chem. Phys. Lett.* 1989, **162**, 165.
12 S. Grimme, J. Antony, S. Ehrlich, and H. Krieg, *J. Chem. Phys.*, 2010, **132**, 154104.
13 A. Schäfer, A. Klamt, D. Sattel, J. C. W. Lohrenz and F. Eckert, *Phys. Chem. Chem. Phys.*, 2000, **2**, 2187.